Journal of Plant Protection Research eISSN 1899-007X

ORIGINAL ARTICLE

Antibacterial activity improvement in a point mutant K45E of the pepper defensin J1-1

Gilberto Andrés Muñoz-Pérez[1], Francisco A. Guillén-Chable[2], Gerardo Corzo[3], Ivan Arenas-Sosa[3], Lucila A. Sánchez-Cach[1], Georgina Estrada[1]*

[1] Unidad de Biología Integrativa, Centro de Investigación Científica de Yucatán, A.C., Yucatán, Mexico

[2] Facultad de Ciencias, Universidad Nacional Autónoma de México, Unidad Multidisciplinaria de Docencia e Investigación, UMIDI-Sisal, Mexico

[3] Instituto de Biotecnología, Universidad Nacional Autónoma de México, Mexico

Vol. 64, No. 4: 287–297, 2024

DOI: 10.24425/jppr.2024.151817

Received: January 27, 2024
Accepted: March 14, 2024
Online publication: October 01, 2024

*Corresponding address:
ginaestapia@yahoo.com.mx

Responsible Editor:
Ammar Al-Farga

Abstract

Plant defensins have attracted much attention in the development of new antimicrobials. Yet the elucidation of their modes of action against bacterial pathogens is still incipient. The available recombinant systems to obtain plant defensin mutants with enhanced or optimized antibacterial activity may help to accelerate the knowledge of their action mechanisms and their applications against pathogens. In this work, the point mutant defensin K45E (J1-1_K45E) was obtained by the same recombinant system as J1-1 defensin. The characterized peptide conserved antibacterial activity against the gram-negative *Pseudomonas aeruginosa* and showed a dose improvement relative to J1-1. Furthermore, the mutant J1-1_K45E exhibited a gain in function against the gram-positive *Staphylococcus aureus.* Finally, to correlate structural changes and antibacterial activity, two properties involved in defensins' modes of action were measured. First, the mutant J1-1_K45E which oligomerizes in a distinct pattern was compared with J1-1 and secondly, J1-1_K45E shows a distinct lipid binding profile because it binds preferentially to phosphatidylserine. Together, our findings support the idea that amino acid sequence variability in plant defensins superfamily can generate major functional changes, and highlight the relevant role of charged residues, beyond the γ-core loop, in the improvement of J1-1 antibacterial activity.

Keywords: antibacterial defensin, gram-positive bacteria, gram-negative bacteria, peptide-lipid interactions, polyclonal antibodies

Introduction

Among multiple sets of molecules produced by plants, plant defensins show antimicrobial activities against human, animal and plant pathogens (Pacheco-Cano *et al.* 2020; Sathoff *et al.* 2020).

According to their subcellular localization, plant defensins are classified as class I or class II. Class I contains a signal peptide and the mature domain, while class II defensins, in addition to the signal peptide and the mature sequence, bear a carboxy-terminal propeptide (Velivelli *et al.* 2018). In nature, these peptides contribute to plant immunity and are induced in response to pathogen attack (Aerts *et al.* 2008; Carvalho and Gomes 2009). Plant defensins are short, cationic, cysteine-rich peptides that fold into the CSαβ 3D structure, which consists of a triple-stranded antiparallel β-sheet and one α-helix stabilized by four disulfides (Lacerda *et al.* 2014).

Class II plant defensins form phospholipid stabilized dimers, considered oligomerization inducers. Some class II defensins dimer stabilization and

oligomerization are lipid concentration dependent processes. Furthermore, oligomeric assemblies are lipid type dependent which might be critical to permeating the membrane and exerting their antimicrobial activity (Kvansakul *et al.* 2016).

Structure-guided mutant peptides have been designed to explore the importance of structural determinants and to find correlations with defensin antifungal activity. Plant defensin interactions with sphingolipids and phospholipids define defensins' mechanisms of action (MOA) on fungal cells, with multiple and varied cellular events as part of cell killing processes. For example, the internalization of MtDef4, from *Medicago truncatula*, depends on the presence of the phosphatidic acid (PA) to exert its antifungal activity on *Fusarium graminearum* and *Neurospora crassa*. Additionally, GluCer is required for RsAFP2 to induce apoptosis, cell wall stress, reactive oxygen species and septin mislocalization in *Candida albicans* (Cools *et al.* 2017).

Recently, several class II defensins in complex with phospholipids have been crystalized and their oligomeric structures are available. These defensin-lipid oligomeric structures have allowed for the analysis of precise molecular interactions namely, protein-lipid interactions and protein-protein interactions in defensin dimers and oligomer interfaces (Poon *et al.* 2014; Kvansakul *et al.* 2016; Järvå *et al.* 2017; Ochiai *et al.* 2020).

Binding to phospholipids involves cationic residues in the interface. For example in *Nicotiana alata* defensin NaD1, the mutant R40E showed reduced binding and oligomerization with PI (4) P compared to the WT. Moreover, the mutant exhibited reduced activity on *Fusarium oxysporum*. In NaD1, R40 is involved in PI (4,5) P2 binding through a network of hydrogen bonds with N-terminus and the γ-core residues (Poon *et al.* 2014).

Additionally, two-mutant peptides, K36E and R39A from NaD1, coordinated the phosphate head group of PA as observed in the NaD1-PA complex. The mutant R39A was unable to form oligomers in the presence of PA. Regarding their antifungal activity against *C. albicans*, both peptides showed higher IC_{50} values (2.5 ± 0.1 μM for K36E and 4.5 ± 0.1 μM for R39A) than WT NaD1 (1.9 ± 0.2 μM) (Järvå *et al.* 2018).

The *Solanum lycopersicum* defensin TPP3 and defensin OsAFP1, from *Oryza sativa*, share a similar dimer arrangement to that observed in the *Nicotiana suaveolens* defensin NsD7 in complex with PA, where the conserved residues that participate in the dimer interface are numbered K47 and C49. The dimer-dimer interface of OsAFP1 K47 coordinates a phosphate ion, probably because this structure was obtained in the absence of phospholipids (Baxter *et al.* 2015; Ochiai *et al.* 2020).

Finally, two TPP3 variants, K6A and K42E, were designed to compare interactions previously described for K4 and R40 residues in NaD1. Both variants were unable to form high-order oligomers in the presence of PI (4,5) P2. Both lost binding to PI (4,5) P2 on lipid strips, and showed a 3-fold reduction in *F. graminearum* hyphal growth inhibition was observed when compared to WT TPP3 (Baxter *et al.* 2015).

Plant antibacterial defensins have the potential of being applied against antibiotic-resistant bacteria, however, a lack of knowledge regarding their MOA delays their use as antibacterial agents (Ishaq *et al.* 2019). In 2016, the World Health Organization (WHO) was requested by member states to create a priority list of antibiotic-resistant bacteria to support research and development of effective drugs (Tacconelli *et al.* 2018). That list included ESKAPE pathogens (*Enterococcus faecium, Staphylococcus aureus, Klebsiella pneumoniae, Acinetobacter baumannii, Pseudomonas aeruginosa,* and *Enterobacter* species). These ESKAPE pathogens are associated with high rates of mortality, diseases, and economic burden in healthcare worldwide (Idris and Nadzir 2023).

The pepper defensin J1-1 was previously obtained in a bacterial expression system in *Escherichia coli*. Recombinant J1-1 is an antibacterial, PA binding peptide, active on gram-negative *Pseudomonas aeruginosa* (Guillén-Chable *et al.* 2017).

Here, we report the functional characterization of the point mutant J1-1_K45E derived from the type I antibacterial defensin J1-1. This point mutant showed a lipid-independent oligomerization, a distinct lipid-binding specificity, and an improved antibacterial activity. Compared to J1-1, the mutant J1-1_K45E improved its antibacterial activity against the human and animal pathogen *P. aeruginosa*, which consisted of a reduced quantity of peptide needed to inhibit bacterial growth. Interestingly, it exhibited activity against *Staphylococcus aureus*. J1-1_K45E also binds to PA, but acquired the ability to bind to phosphatidylserine (PS) *in vitro*. Yet, J1-1_K45E exhibited differences in its oligomerization pattern compared to J1-1, but neither J1-1 nor J1-1_K45E oligomerize in a PA concentration dependent manner.

Materials and Methods

3D-structure model of dimers

The 3D structural model of J1-1 mature peptide as a monomer was obtained by homology modeling in Modeller software (Fiser and Šali 2003) using the Protein Data Bank (PDB) ID 2LR3 (MtDef4 defensin) as a template. The 3D models of dimers were generated using PDB file 5KK4 (NsD7 defensin) as

template. The molecular surface electrostatic potential of both J1-1 and J1-1_K45E mature peptides were obtained by PyMOL using the software default settings.

Physicochemical characteristics such as molecular weight, isoelectric point, total charge and grand average of hydropathicity (GRAVY) index score of both peptide sequences J1-1 and J1-1_K45E were *in silico* predicted by using ProtParam and Peptide Calculator from Expasy (Gasteiger *et al.* 2003; Gasteiger *et al.* 2005).

Bacterial strains, enzymes and plasmids

Escherichia coli DH5α and *E. coli* Origami (DE3) strains were used for plasmid propagation and recombinant protein expression, respectively. pGEM-TEasy (Promega Biotech, United States) and pQE30 (QIAGEN) plasmids were the cloning and expression vector, respectively, for the J1-1_K45E gene. Bacterial pathogenic strains *S. aureus* ATCC 29213 and *P. aeruginosa* ATCC 27853 were purchased from the American Type Culture Collection (ATCC) through The Global Bioresource Center™.

Expression and purification of J1-1_K45E

A mutant gene of the previously reported J1-1 was obtained by PCR from *Capsicum chinense* Jacq genomic DNA using specific primers. A reverse primer was designed to introduce a point mutation in the K45E in J1-1 mature peptide sequence. The reverse primer sequence was 5′GCT AAT TAA GCT TGG CTG CAG TTA AGC ACA GGG CTC 3′. J1-1_K45E gene cloning was performed by introducing *Bam HI* and *Pst I* sites at 5′and 3′, respectively. The obtained plasmid construct in the expression vector pQE30 or pQE30_J1-1_K45E (Guillén-Chable *et al.* 2017) was confirmed by sequencing. The recombinant expression and purification of recombinantly expressed J1-1_K45E, was performed by affinity chromatography using nickel-nitrilotriacetic acid (Ni-NTA) under denaturant conditions (Qiagen) and reverse-phase High Performance Liquid Chromatography (rpHPLC). Briefly, a semi-preparative C_{18} column (5 C_{18}MS, 10 × 250 mm Nacalai-Tesque Japan) was run from solvent A (0.1 and trifluoroacetic acid (TFA) in water) to solvent B (0.1 and TFA in acetonitrile (ACN)) using a gradient that started after 10 min from 10 to 100% of solvent B in 30 min at a flow of 1.5 ml · min^{-1}. After collecting J1-1_K45E manually, it was vacuum dried and solubilized in sterile H_2O. Pure J1-1_K45E and J1-1 were used for the protein-lipid interaction assay, protein cross-linking and antibacterial activity assays.

Peptide analysis by SDS-PAGE and Western Blot

Both J1-1_K45E and J1-1 were visualized by sodium dodecyl sulfate-poliacrylamide gel electrophoresis (SDS-PAGE) under reducing and denaturant conditions. The polyacrylamide gels were stained with Coomassie R250 Brilliant Blue solution for 30 min. The destaining solution was a mixture of acetic acid and methanol. The molecular mass markers used for SDS-PAGE and Western Blot were from either Sigma (Color Markers Wide Range, Sigma-Aldrich Cat. 3437; Broad-Range SDS-PAGE Standards Sigma-Aldrich Cat.1610317) or Thermo (PageRuler™ Prestained Protein Ladder, Thermo Scientific™).

To observe differences in the cross-linking profile of the recombinant peptides, identical samples were used in standard SDS-PAGE and Western Blot (WB) (Mahmood and Yang 2012). The protein detection was performed using previously obtained polyclonal rabbit antibodies anti-J1-1 (Guillen-Chablé *et al.* 2017). After SDS-PAGE, proteins were transferred to PVDF (polyvinylidene fluoride, Immobilon®-P Millipore) membranes. Immunodetection of oligomeric complexes of both peptides were performed by using polyclonal antibodies anti-J1-1 (1 : 10,000 dilution). Then anti-rabbit horseradish peroxidase (HRP)-coupled-IgG was used as a secondary antibody (Sigma-Aldrich Cat. 32160702). Chemioluminiscence detection and image acquisition were obtained in a ChemiDoc™MP Imaging System BIO-RAD (Mahmood and Yang 2012).

Protein cross-linking

Cross-linking reactions were conducted in a volume of 50 µl containing 1 mg · ml of J1-1 or J1-1_K45E, 5 mM bis(sulfosuccinimidyl) suberate (BS^3) (Islam *et al.* 2017). The modified conditions were as follows, defensins were incubated in the presence or absence of 447.8 µM PA and 150 mM of NaCl in water, at room temperature. After 30 min of incubation, 5 µl Tris 500 mM was used to stop the reaction. Protein samples were visualized using 12 µl of the protein cross-linking reactions, boiled for 5 min at 95°C under reducing and denaturing conditions and loaded into SDS-PAGE lanes and ran at 120 V (Mini PROTEAN tetra Cell chamber BioRad™). Proteins were stained with Coomassie blue or transferred to PVDF membranes for Western Blot analysis.

Antibacterial activity

The bacterial strains, *S. aureus* ATCC 29213 and *P. aeruginosa* ATCC 27853, were cultured with J1-1_K45E in broth microdilution assay as previously described by Guillén-Chable *et al.* (2017) with some

modifications. Briefly, modifications consisted of using ½ Mueller-Hinton broth (MHB) (BD Biosciences, Sparks, Md.) instead of MH medium. It was performed as a consequence of the observed aggregation in solution at peptide concentrations of 125 µg · ml^{-1} and 250 µg · ml^{-1} in MHB. The peptide J1-1_K45E was diluted in sterile ½ MHB in 96-well microtiter Costar® culture plates (Sigma-Aldrich) to a final volume of 100 µl, *i.e.*, 50 µl of bacterium in ½ MHB and 50 µl of the recombinant peptide in sterile water containing the corresponding peptide concentration. The bacterial strains were initially cultured in ½ MHB to reach values between 0.08 and 0.1 absorbance units at 600 nm. Then, cultures were diluted 1 : 100 with sterile ½ MHB. Fifty µl of these dilutions were dispensed into each plate well, and immediately 50 µl of a two-fold final concentration of the peptide J1-1_K45E solution was added to reach a final volume of 100 µl per well. Culture plates were incubated at 37°C for 18 h. Absorbance at 600 nm was measured using a Sunrise™ plate reader Tecan Group Ltd. (San Jose, CA, USA). Experiments were conducted with gentamicin as the control and without antibiotic to calculate maximum growth. Replicates were n = 4. Next, Colony Forming Units (CFU) assays were performed as follows, a volume of 10 µl from overnight microdilution cultures at peptide concentrations: 250, 125, 62.5, 31.25 and 15.62 µg · ml^{-1}, as well as the positive or negative control were taken and serially diluted (6-fold). Finally, 15 µl of each dilution was plated onto ½ MH-agar and incubated for 18 h at 37°C (n = 2). To obtain the bacterial inhibition percentages, CFU for *P. aeruginosa* and *S. aureus* were calculated according to the following formula (Scilletta *et al.* 2021):

$$\text{CFU} = \frac{\text{Number of colonies} \times \text{Dilution factor}}{\text{Platet volume in ml}}.$$

Peptide-lipid binding

In vitro peptide-lipid interactions were analyzed as previously reported elsewhere (Poon *et al.* 2014). Briefly, J1-1_K45E lipid interactions using P-6001 phosphatidylinositol phosphate (PIP) strips (Echelon Biosciences, Salt Lake City, UT, USA) were used together with HRP-coupled anti-rabbit antibodies as secondary antibodies (Sigma-Aldrich 32160702, diluted 1 : 10,000). The membrane was incubated for 20 min, and after two washing steps with 5 ml of Tris buffered saline plus Tween 20 (TBS-T), treated with the Immobilon Western Chemiluminescent HRP Substrate (Millipore Co.) following the manufacturer's instructions. Peptide-lipid binding was detected by chemioluminiscence and documented in a ChemiDoc™MP Imaging System (BIORAD).

Results

Cloning of J1-1_K45E gene into the pQE30 expression plasmid

The vector pQE30 was used to express the *Capsicum chinense* defensin mutant gene J1-1_K45E in *E. coli* Origami (DE3) strain. The expression plasmid contains a T5 promoter to be induced by isopropyl thiogalactoside (IPTG) which is added to the culture medium for protein expression. The expressed recombinant defensin bear an N-terminal 6xHis tag to facilitate the purification by affinity chromatography, followed by a sequence that encodes the 4 amino acids (IEGR) that serve as a cut site for Factor Xa protease to release, if necessary, the J1-1_K45E mature peptide from the 6xHis-tag. The correct reading frame and restriction sites in the new pQE30J1-1_K45E plasmid were confirmed. Figure 1A shows the 3D structure model of the monomeric defensin J1-1 and the putative PA and PIP2 binding residues. Figure 1B shows the J1-1_K45E fusion protein format and its amino acid sequence, and Figure 1C shows theoretical biophysical values of J1-1 and J1-1_K45E.

Recombinant expression and J1-1_K45E purification

The pQE30J1-1_K45E plasmid, previously sequenced, was used to transfect the expression *E. coli* Origami (DE3) strain. A single ampicillin-resistant colony was used to inoculate 1 L of LB medium flask containing ampicillin at 100 µg · ml-1. After induction and then protein purification by affinity chromatography, the expression of J1-1_K45E was observed by SDS-PAGE (Fig. 2). Intense protein bands of J1-1_K45E ~7 kDa (monomeric, I) in multimeric forms were observed, that is, protein bands of ~ 14 and ~21 kDa corresponding to dimers and trimers were observed. Also, other multimeric forms with larger molecular mass were visible (Fig. 2).

After nickel affinity chromatography purification, the main fractions were injected into the C18 column for a rpHPLC purification. The resulting chromatogram of this purification is shown in Figure 3. Mass spectrometric analysis of J1-1_K45E, collected at a retention time (RT) of 26.6 min, showed a molecular mass of 7,044.8 Da. The fraction with RT of 11.8 min corresponds to solution salts or other low molecular mass components from the affinity chromatography elution fractions.

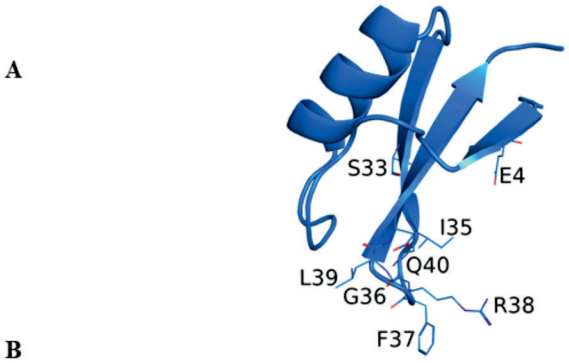

B

J1-1_K45E MRGSHHHHHHGS*IEGR*KICEALSGNFKGLCLSSRDCGNVCRREGFTDGSCIGFRLQCFCT*E*PCA

6xHis-Tag Fxa

1 10 20 30 40 48

C

Peptide	Molecular weight	Isoelectric point	Total charge	GRAVY
J1-1	7,050.05	8.75	+4	−0.433
J1-1_K45E	7,050.99	8.19	+2.1	−0.427

Fig. 1. Structure model and properties of recombinant J1-1_K45E. A) Cartoon representation showing the side chains reported to interact with PA and PIP2; B) Amino acid sequence in recombinant J1-1_K45E, side chains shown on A are highlighted with asterisks Double lines indicate PIP2-binding amino acids; C) Comparison of biophysical values of both defensins

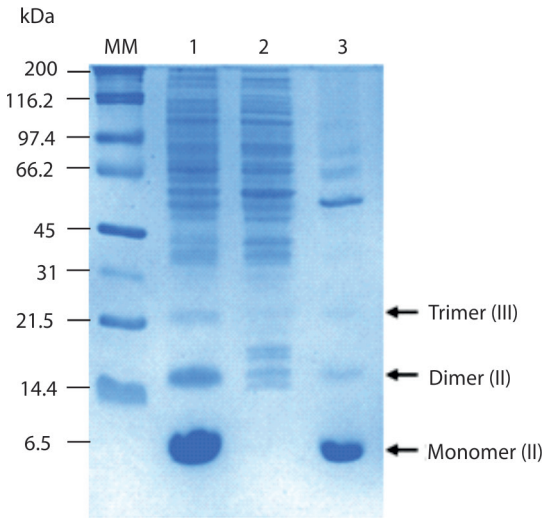

Fig. 2. Affinity Chromatography Purification of the recombinant J1-1_K45E. MM – molecular weight marker; 1 – GdnHCl solubilized inclusion bodies; 2 – flow-through; 3 – protein elution with imidazole 0.7 M. Black arrows indicate the monomers (I), dimers (II) and trimers (III)

Immunodetection of recombinant peptides

After rpHPLC purification, J1-1 and J1-1K_45E were analyzed by SDS-PAGE and by WB (Fig. 4). Furthermore, to observe differences in the oligomeric profile between J1-1 and J1-1K_45E, anti-J1-1 polyclonal antibodies were used to observe oligomer formation before and after cross-linking reaction. Before cross-linking, the J1-1 antibodies were able to recognize the recombinant mutant J1-1_K45E of the monomers, dimers, and trimers (Fig. 4).

Dimeric 3D models and surface potential

The homology of a 3D model of J1-1 was obtained to predict the structure of defensins and contribute to the analysis of structure-function relationship. The 3D model of J1-1 was built on the structural template from *Medicago truncatula*, MtDef4 (PDB: 2LR3) with a sequence identity of 48.9%. The structure model of J1-1 contained a conserved triple-stranded β-sheet (β1-β3) and the α-helix, illustrating the conserved plant defensins CSαβ fold (Fig. 5A). To observe the effect of the charge inversion in J1-1_K45E in comparison to J1-1, the molecular surface electrostatic potential of dimer analysis was performed using the modeled peptides in PyMOL. The analysis showed the expected increment in the negative surface area, located as a negatively charged patch shown in red in the J1-1_K45E dimer (Fig. 5C) and absent in J1-1 dimer (Fig. 5B).

Oligomerization of recombinant defensins

The capability of J1-1_K45E and J1-1 to oligomerize in solution was investigated using the BS^3 chemical cross-linker, in the presence or absence of PA and NaCl

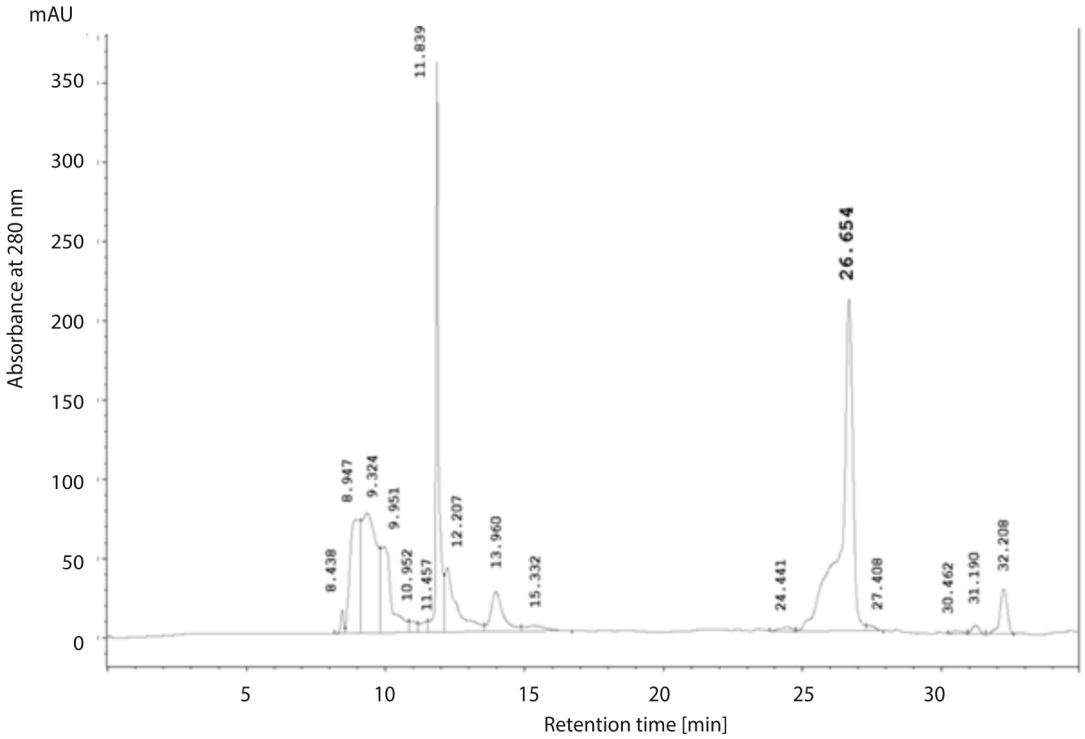

Fig. 3. rpHPLC chromatogram of recombinant J1-1_K45E. A fraction with RT 26.654 min, was further analyzed by mass spectrometry to confirm mutant defensin identity. The phase gradient was from 10 to 100 and ACN in 30 min. Nickel affinity purified fractions of J1-1_K45E were loaded into the C_{18} column

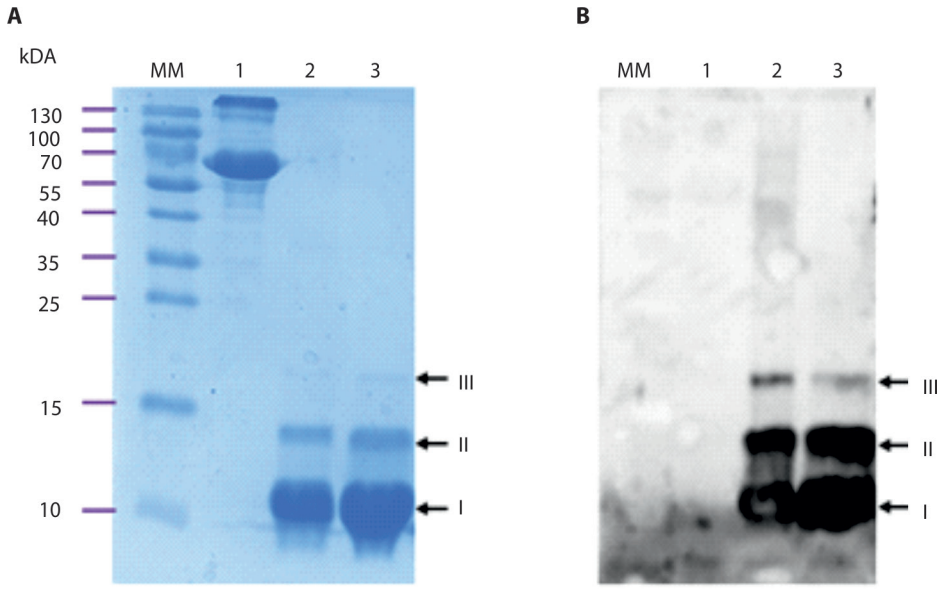

Fig. 4. Detection of J1-1 and J1-1K45E by SDS-PAGE and WB. A) SDS-PAGE, lane 1, BSA, lane 2, recombinant J1-1, and lane 3 recombinant J1-1_K45E; B) The Western Blot is a replica of the SDS-PAGE from Figure 4A where proteins were transferred to a PVDF membrane and it was immunodetected by anti-J1-1 polyclonal antibodies. Black arrows indicate the monomers (I), dimers (II) and trimers (III)

(Fig. 6). Oligomers in the presence or absence of PA or NaCl were observed for J1-1 and J1-1_K45E recombinant peptides in Coomassie blue stained SDS-PAGE. Protein bands around 7, 14, ~21, ~28 and ~35 kDa were present, which would be equivalent to monomers, dimers, trimers, tetramers and pentamers of each peptide. It is worth mentioning that rpHPLC purified peptides, without any treatment, showed specific laddering patterns. The most abundant bands were the smaller oligomers observed, corresponding to monomers, dimers and trimers (Fig. 6A and 6C). In the control oligomerization patterns (rpHPLC purified peptide), tetramers

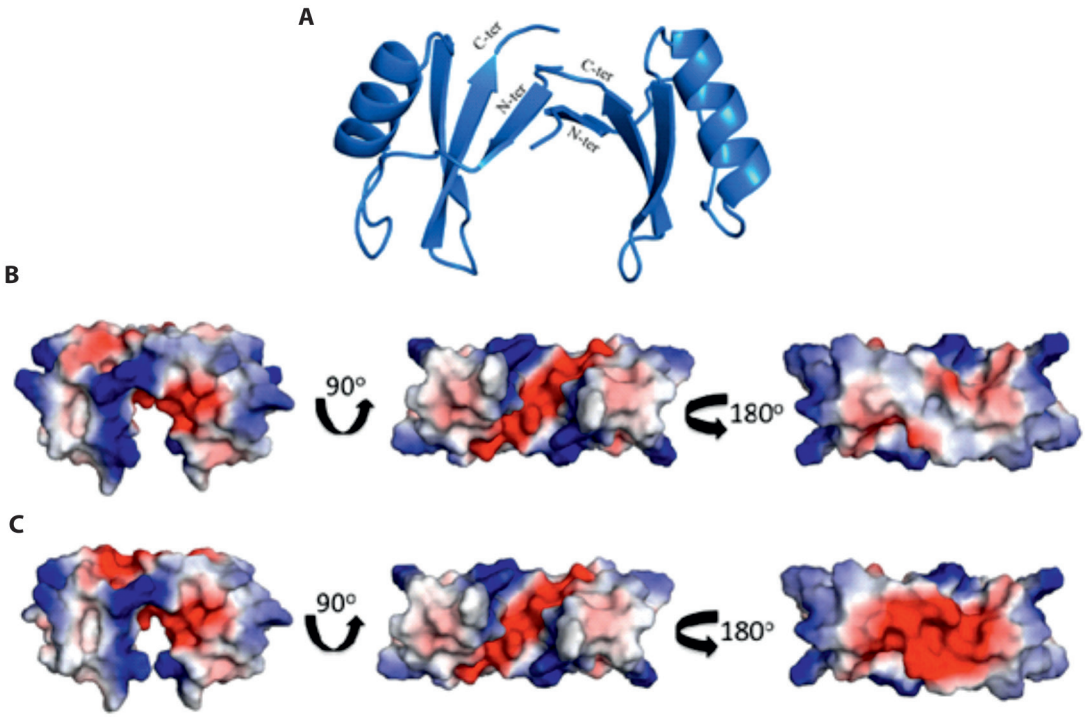

Fig. 5. J1-1 and J1-1_K45E dimers. A) 3D structure of J1-1 dimer obtained by homology modeling. B) J1-1 dimer molecular surface electrostatic potential and C) J1-1_K45E dimer molecular surface electrostatic potential. Models were generated using PyMOL with default settings. The template was the plant defensin NsD7 (PDB: 5KK4)

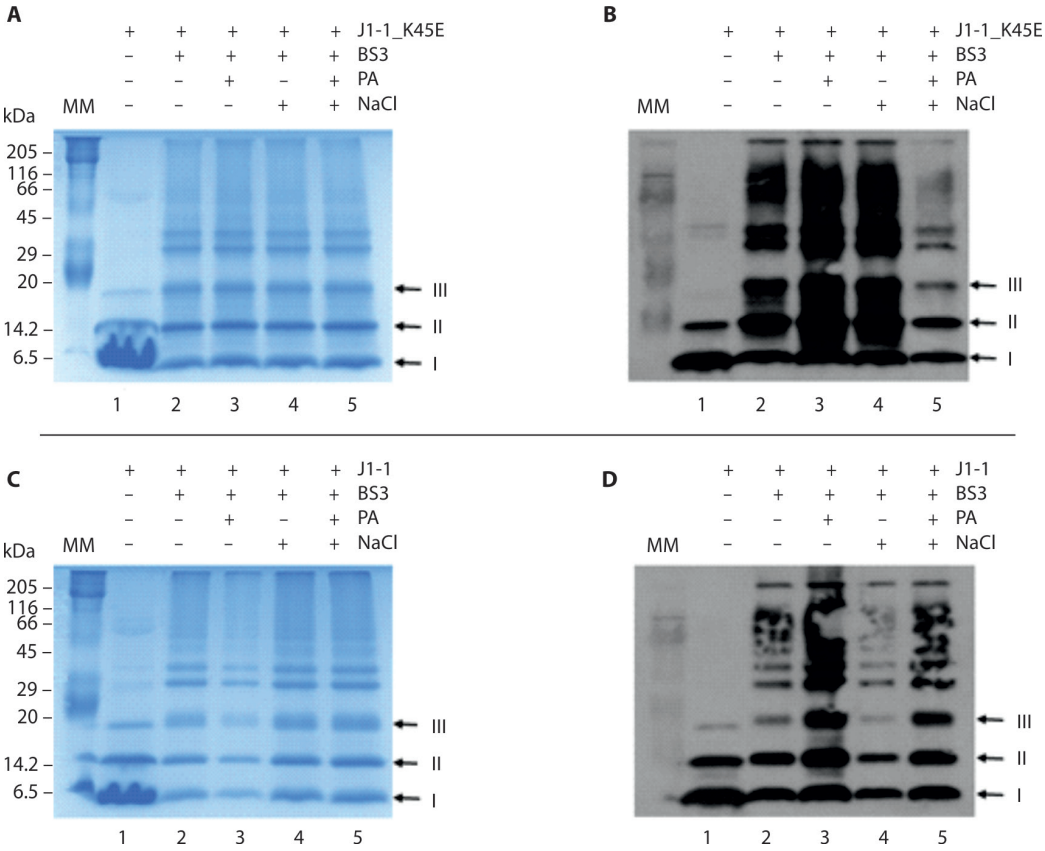

Fig. 6. J1-1 and J1-1_K45E cross-linking and immunodetection. A) SDS-PAGE of J1-1_K45E and cross-linking products stained with Coomassie blue; B) WB with J1-1_K45E cross-linking products in reactions with or without PA or NaCl; C) SDS-PAGE of J1-1 and cross-linking products stained with Coomassie blue and D), WB with J1-1 cross-linking products, reactions, with or without PA or NaCl. Lanes from 1 to 5 indicate: + means added reagent, and – means non-added reagent. Arrows indicate: monomers (I), dimers (II), and trimers (III)

and pentamers appeared after BS^3 cross-linking for both, J1-1_K45E and J1-1. It was noticed that oligomers under 205 kDa for J1-1 were present when NaCl was added in the cross-linking reaction (Fig. 6C, lanes 4 and 5). For J1-1_K45E, a clear difference in larger molecular mass oligomers was not observed between the different reaction conditions in SDS-PAGE (Fig. 6A, lanes 2 to 5). To better observe differences in larger mass oligomerization patterns, the cross-linked peptides J1-1_K45E (Fig. 6B) and J1-1 (Fig. 6D) were analyzed by WB, with anti-J1-1 polyclonal antibody. As in SDS-PAGE. J1-1 formed high mass oligomers in the presence or absence of PA, with no noticeable effect in cross-linking reactions with or without NaCl (Fig. 6D, lanes 3 to 5) The same pattern is observed in lane 2 which only contains J1-1 cross-linked with BS^3. J1-1_K45E, was detected in a different laddering pattern that is evidence of a change in higher mass oligomers. Undefined bands were mainly observed in reactions conducted with PA and NaCl (Fig. 6B, lanes 3 and 4). On the other hand, cross-linked J1-1_K45E showed oligomers without PA or NaCl that are immunodetected in a similar laddering pattern (Fig. 6B, lane 2).

Antibacterial activity

Antibacterial activity of J1-1_K45E was evaluated on *P. aeruginosa* ATCC 27853 and *S. aureus* ATCC 29213 results are shown in Figure 7. Although the absorbance at 600 nm was measured it was not conclusive because at high concentrations peptide aggregation interfered with absorbance due to bacterial growth. Yet, total inhibition of cell growth was obtained at 125 μg · ml^{-1} for *P. aeruginosa* and 250 μg · ml^{-1} for *S. aureus*. These values were confirmed by performing CFU plate assays. The CFU remaining values for *P. aeruginosa* were in the range of 3.3×10^8 to 2.3×10^5 at 15.6 μg · ml^{-1} and 62.5 μg · ml^{-1}, respectively, of J1-1_K45E, compared to the positive control value of 1.1×10^9 CFU · ml^{-1}. In contrast, CFU for *S. aureus* were 3.3×10^8 CFU · ml^{-1} at 15.6 μg · ml^{-1} and 6.7×10^6 CFU · ml^{-1} at a peptide concentration of 125 μg · ml^{-1}. Bacterial growth control (without peptide or gentamicin) was 4.7×10^8 CFU · ml^{-1}.

J1-1 K45E *in vitro* lipid binding

The lipid binding profile of recombinant J1-1 was previously reported. J1-1 binds to phosphoinositides (PIs): mono, bisphosphates and trisphosphates, and PA *in vitro* (Guillén-Chable *et al.* 2017). In this work, the mutant J1-1_K45E lipid binding profile was obtained *in vitro* with PIP Strips. Recombinant defensin J1-1_K45E exhibited a single amino acid charge inversion in comparison to J1-1 (K 45 for an E), but a reduction in cationic charge of two units. Interestingly, J1-1_K45E bound to PtdIns (4,5) P2, PtdIns (3,4,5) P3, PA and PS on P-6001 strip. In contrast, J1-1_K45E did not bind either mono-PIs, PtdIns (3,4) P2 or PtdIns (3,5) P2. Identical results from two independent assays are shown in Figure 8. Remarkably, J1-1_K45E bound to PS.

Discussion

In this work, we reported the purification and characterization of the point mutant J1-1_K45E. This point mutant had a Glu residue instead of a Lys residue at

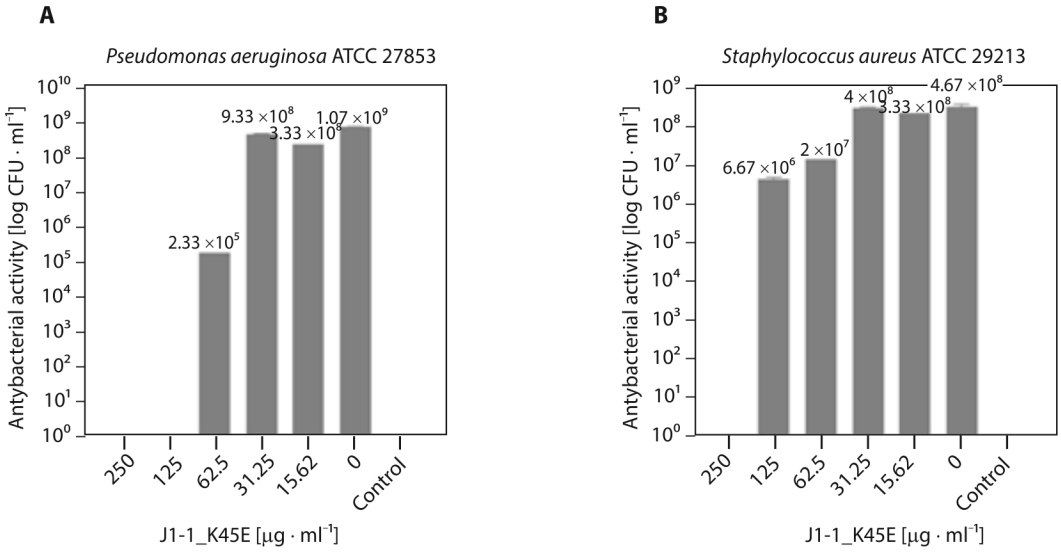

Fig. 7. Antibacterial activity of J1-1_K45E against A) *Pseudomonoas aeruginosa* ATCC 27853, control – gentamicin 4 μg · ml^{-1} and B) *Staphylococcus aureus* ATCC 29213, control – gentamicin 16 μg · ml^{-1}; CFU · ml^{-1} after18 h in 37°C

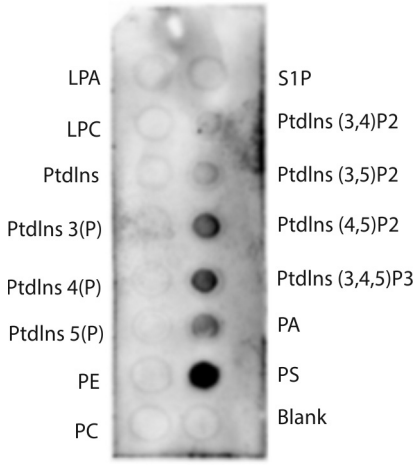

Fig. 8. J1-1_K45E lipid binding. J1-1_K45E bound to PtdIns (4,5) P2, PtdIns (3,4,5) P3, PA and PS *in vitro*

position 45 of mature J1-1. This mutant peptide was successfully expressed and purified as well as J1-1. The point mutation changed the total charge from +4 in J1-1, to +2.1 in J1-1_K45E. It is already known that under physiological salt concentrations the effectiveness of antimicrobial peptides (AMPs) might be affected by reducing electrostatic interactions between the cationic amino acids and anionic surface of the microbial membrane and the presence of cations, such as Na^+ or K^+, disturbing the protein-protein interactions, which would directly affect the oligomer formation (Kerenga *et al.* 2019). Lipid-dependent oligomerization has been described as a key event in the mechanism of action of plant defensins on fungal cells. Disruption of the oligomer formation is associated with a reduction in the biological activity of plant defensins (Poon *et al.* 2014; Kvansakul *et al.* 2016; Järvå *et al.* 2018). In the SDS-PAGE analysis of proteins stained with Coomassie blue we observed very similar peptide patterns before and after cross-linking reactions. To observe oligomers under several conditions, such as NaCl presence, PA presence or both, different cross-linking reactions were designed. Detection of low quantities of peptides were achieved by WB, after reducing and denaturating conditions and specific patterns were identified for each peptide. We observed that the oligomer patterns change due to mutation K45E, and that the capacity to oligomerize is not dependent on the NaCl or presence of PA.

To our knowledge this is the first report that points out the enhancement of antibacterial activity by reducing the cationicity of a plant defensin. J1-1_K45E showed antibacterial activity in the two strains tested. In a previous work on J1-1, the MIC for *P. aeruginosa* was determined in 250 $\mu g \cdot ml^{-1}$ but it did not inhibit *S. aureus* at the same concentration (Guillén-Chable *et al.* 2017). In this work, an enhanced antibacterial activity on *P. aeruginosa* was observed at a peptide concentration of 125 $\mu g \cdot ml^{-1}$ and unexpectedly, this point mutant killed *S. aureus* at 250 $\mu g \cdot ml^{-1}$. The antibacterial activity of J1-1_K45E might be influenced by the global electrostatic charge, but also it might be related to the lipid selectivity or to the J1-1_K45E oligomerization pattern. It is important to highlight that antimicrobial mechanisms described on fungal cells are different, even when a distinct susceptible fungal genus is described. Furthermore, antibacterial defensins have been reported to bind not only to membrane lipids, but also to ligands such as cell wall constituents, enzymes or intracellular targets as DNA and ribosomes have been identified (Velivelli *et al.* 2018; Sathoff *et al.* 2019).

J1-1_K45E bound to PtdIns (4,5) P2, PtdIns (3,4,5) P3, PA and PS *in vitro*. Interestingly, J1-1 did not bind to PS, but as previously reported, it bound to mono-PtdIns, tris-PtdIns, PA and also to bis-PtdIns (3,4) P2 and PtdIns (3,5) P2. Such differences in lipid-binding, suggest a role of the residue K45 in selectivity related to charge or size of the lipid head group that, when substituted by an opposite charged side chain, could bind PS. This is important in the first step for membrane interaction or it is necessary to cross the membrane to reach intracellular targets as described for antifungal plant defensins (Poon *et al.* 2014; Baxter *et al.* 2015; Järvå *et al.* 2018). Lipids in bacterial membranes are important structural and functional constituents, and are targets of several types of AMP. Membrane lipids perform variable roles in cellular events as structural components or as signaling molecules (Tam *et al.* 2015). In this context, the binding of J1-1_K45E to PS is relevant due to its physiological cellular functions described. Phosphatidylserine (PS) is an anionic lipid found on cellular membranes, that under homeostatic conditions is typically restricted to the inner leaflet of the plasma membrane. It has a key role in conditions such as: apoptosis, protist apoptotic mimicry which is a condition where pathogens, expose PS on the membrane to enter into the host cells to deploy its virulence, and PS externalization in some cancer cell lines (Calianese and Birge 2020). In this sense, further work is needed to explore the J1-1_K45E binding to cancer cells or to evaluate its effect on other pathogens in apoptotic mimicry.

Conclusions

In conclusion, the positive charge of the Lys residue in position 45 was a determinant for oligomerization and lipid-binding of J1-1. Interestingly, the residue Glu 45 enhanced peptide antibacterial activity on *P. aeruginosa* and also conferred activity on *S. aureus* that was not previously observed in J1-1. This work highlights the

role of the amino acid K45 as a key structural determinant for head group phospholipid interactions and the role of K45 in J1-1 oligomerization. On the other hand, the improved antibacterial activity of J1-1_K45E is contrary to the accepted idea that more positively charged plant defensins exert better antimicrobial activity. More structure-function studies considering dimeric or oligomeric forms of these peptides are necessary to accurately elucidate antibacterial plant defensins mode of action.

Acknowledgements

This work was supported partially by CONAHCyT 303045. GAMP received the CONAHCyT scholarship No. 775005.

References

Aerts A.M., François I.E.J.A., Cammue B.P.A., Thevissen K. 2008. The mode of antifungal action of plant, insect and human defensins. Cellular and Molecular Life Sciences 65 (13): 2069–2079. DOI: https://doi.org/10.1007/s00018-008-8035-0

Baxter A.A., Richter V., Lay F.T., Poon I.K.H., Adda C.G., Veneer P.K., Phan T.K., Bleackley M.R., Anderson M.A., Kvansakul M., Hulett M.D. 2015. The tomato defensin TPP3 binds phosphatidylinositol (4,5)-bisphosphate via a conserved dimeric cationic grip conformation to mediate cell lysis. Molecular and Cellular Biology 35 (11): 1964–1978. DOI: https://doi.org/10.1128/MCB.00282-15

Calianese D.C., Birge R.B. 2020. Biology of phosphatidylserine (PS): Basic physiology and implications in immunology, infectious disease, and cancer. Cell Communication and Signaling 18 (1): 41. DOI: https://doi.org/10.1186/s12964-020-00543-8

Carvalho A. de O., Gomes V.M. 2009. Plant defensins – prospects for the biological functions and biotechnological properties. Peptides 30 (5): 1007–1020. DOI: https://doi.org/10.1016/j.peptides.2009.01.018

Cools T.L., Struyfs C., Cammue B.P., Thevissen K. 2017. Antifungal plant defensins: Increased insight in their mode of action as a basis for their use to combat fungal infections. Future Microbiology 12: 441–454. DOI: https://doi.org/10.2217/fmb-2016-0181

Fiser A., Šali A. 2003. MODELLER: generation and refinement of homology-based protein structure models. Methods in Enzymology 374: 461–491. MODELLER. Retrieved https://salilab.org/modeller/

Gasteiger E., Gattiker A., Hoogland C., Ivanyi I., Appel R.D., Bairoch A. 2003. ExPASy: the proteomics server for in-depth protein knowledge and analysis. Nucleic Acids Research 31: 3784–3788. DOI: https://web.expasy.org/protparam/

Gasteiger E., Hoogland C., Gattiker A., Duvaud S., Wilkins M.R., Appel R.D., Bairoch A. 2005. Protein identification and analysis tools on the expasy server. The Proteomics Protocols Handbook, Humana Press, 571–607.

Guillén-Chable F., Arenas-Sosa I., Islas-Flores I., Corzo G., Martinez-Liu C., Estrada G. 2017. Antibacterial activity and phospholipid recognition of the recombinant defensin J1-1 from *Capsicum* genus. Protein Expression and Purification 136: 45–51. DOI: https://doi.org/10.1016/j.pep.2017.06.007

Idris F.N., Nadzir M.M. 2023. Multi-drug resistant ESKAPE pathogens and the uses of plants as their antimicrobial agents. Archives of Microbiology 205 (4): 115. DOI: https://doi.org/10.1007/s00203-023-03455-6

Ishaq N., Bilal M., Iqbal H.M.N. 2019. Medicinal potentialities of plant defensins: a review with applied perspectives. Medicines 6 (1): 29. DOI: https://doi.org/10.3390/medicines6010029

Islam K.T., Velivelli S.L.S., Berg R.H., Oakley B., Shah D.M. 2017. A novel bi-domain plant defensin MtDef5 with potent broad-spectrum antifungal activity binds to multiple phospholipids and forms oligomers. Scientific Reports 7 (1) DOI: https://doi.org/10.1038/s41598-017-16508-w

Järvå M., Lay F.T., Hulett M.D., Kvansakul M. 2017. Structure of the defensin NsD7 in complex with PIP2 reveals that defensin: lipid oligomer topologies are dependent on lipid type. FEBS Letters 591 (16): 2482–2490. DOI: https://doi.org/10.1002/1873-3468.12761

Järvå M., Lay F.T., Phan T.K., Humble C., Poon I.K.H., Bleackley M.R., Anderson M.A., Hulett M.D., Kvansakul M. 2018. X-ray structure of a carpet-like antimicrobial defensin-phospholipid membrane disruption complex. Nature Communications 9 (1): 1962. DOI: https://doi.org/10.1038/s41467-018-04434-y

Kerenga B.K., McKenna J.A., Harvey P.J., Quimbar P., Garcia-Ceron D., Lay F.T., Phan T.K., Veneer P.K., Vasa S., Parisi K., Shafee T.M.A., van der Weerden N.L., Hulett M.D., Craik D.J., Anderson M.A., Bleackley M.R. 2019. Salt-Tolerant Antifungal and Antibacterial Activities of the Corn Defensin ZmD32. Frontiers in Microbiology 10. DOI: https://www.frontiersin.org/articles/10.3389/fmicb.2019.00795

Kvansakul M., Lay F.T., Adda C.G., Veneer P.K., Baxter A.A., Phan T.K., Poon I.K.H., Hulett M.D. 2016. Binding of phosphatidic acid by NsD7 mediates the formation of helical defensin-lipid oligomeric assemblies and membrane permeabilization. Proceedings of the National Academy of Sciences of the United States of America 113: 11202–11207. DOI: https://doi.org/10.1073/pnas.1607855113

Lacerda A., Vasconcelos É., Pelegrini P., Grossi-de-Sa M.F. 2014. Antifungal defensins and their role in plant defense. Frontiers in Microbiology 5: 116. DOI: https://www.frontiersin.org/articles/10.3389/fmicb.2014.00116

Mahmood T., Yang P.C. 2012. Western Blot: technique, theory, and trouble shooting. North American Journal of Medical Sciences 4 (9): 429–434. DOI: https://doi.org/10.4103/1947-2714.100998

Ochiai A., Ogawa K., Fukuda M., Suzuki M., Ito K., Tanaka T., Sagehashi Y., Taniguchi M. 2020. Crystal structure of rice defensin OsAFP1 and molecular insight into lipid-binding. Journal of Bioscience and Bioengineering 130: 6–13. DOI: https://doi.org/10.1016/j.jbiosc.2020.02.011

Pacheco-Cano R.D., Salcedo-Hernández R., Casados-Vázquez L.E., Wrobel K., Bideshi D.K., Barboza-Corona J.E. 2020. Class I defensins (BraDef) from broccoli (*Brassica oleracea* var. *italica*) seeds and their antimicrobial activity. World Journal of Microbiology & Biotechnology 36 (2): 30. DOI: https://doi.org/10.1007/s11274-020-2807-6

Poon I.K., Baxter A.A., Lay F.T., Mills G.D., Adda C.G., Payne J.A., Phan T.K., Ryan G.F., White J.A., Veneer P.K., van der Weerden N.L., Anderson M.A., Kvansakul M., Hulett M.D. 2014. Phosphoinositide-mediated oligomerization of a defensin induces cell lysis. eLife 3: e01808. DOI: https://doi.org/10.7554/eLife.01808

Sathoff A.E., Lewenza S., Samac D.A. 2020. Plant defensin antibacterial mode of action against *Pseudomonas* species. BMC Microbiology 20 (1): 173. DOI: https://doi.org/10.1186/s12866-020-01852-1

Sathoff A.E., Velivelli S., Shah D.M., Samac D.A. 2019. Plant defensin peptides have antifungal and antibacterial activity

against human and plant pathogens. Phytopathology 109 (3): 402–408. DOI: https://doi.org/10.1094/PHYTO-09-18-0331-R

Scilletta N.A., Pezzoni M., Desimone M.F., Soler-Illia G.J.A.A., Bellino M.G., Catalano P.N. 2021. Determination of antibacterial activity of film coatings against four clinically relevant bacterial strains. Bio-Protocol 11 (2): e3887. DOI: https://doi.org/10.21769/BioProtoc.3887

Schrödinger L., DeLano W. 2020. PyMOL. Retrieved from http://www.pymol.org/pymol

Tacconelli E., Carrara E., Savoldi A., Harbarth S., Mendelson M., Monnet D.L., Pulcini C., Kahlmeter G., Kluytmans J., Carmeli Y., Ouellette M. Discovery, research, and development of new antibiotics: the WHO priority list of antibiotic-resistant bacteria and tuberculosis. 2018. The Lancet Infectious Diseases 18 (3): 318–327. DOI: https://doi.org/10.1016/S1473-3099(17)30753-3

Tam J.P., Wang S., Wong K.H., Tan W.L. 2015. Antimicrobial Peptides from Plants. Pharmaceuticals 8 (4): 711–757. DOI: https://doi.org/10.3390/ph8040711

Velivelli S.L.S., Islam K.T., Hobson E., Shah D.M. 2018. Modes of action of a bi-domain plant defensin mtdef5 against a bacterial pathogen *Xanthomonas campestris*. Frontiers in Microbiology 9. DOI: https://www.frontiersin.org/articles/10.3389/fmicb.2018.00934